mM caused responses in oocytes expressing mGluR1α (Fig. 5). It is possible that the activation of mGluR1α would be triggered by the fluctuation of local $[Ca^{2+}]_o$ in the synaptic cleft.

Thus, mGluRs 1α, 5, and 3 but not mGluR2 are activated by $Ca^{2+}{}_o$ at physiological concentrations, and a single amino acid residue determines the sensitivity to $Ca^{2+}{}_o$. Also, the $Ca^{2+}{}_o$-sensing function of mGluR1α can play a role in generating morphological changes in transfected cells.

REFERENCES AND NOTES

1. H. Sugiyama, I. Ito, C. Hirono, *Nature* **325**, 531 (1987); M. Masu, Y. Tanabe, K. Tsuchida, R. Shigemoto, S. Nakanishi, *ibid.* **349**, 760 (1991); Y. Tanabe, M. Masu, T. Ishii, R. Shigemoto, S. Nakanishi, *Neuron* **8**, 169 (1992); T. Abe *et al.*, *J. Biol. Chem.* **267**, 13361 (1992); Y. Nakajima *et al.*, *ibid.* **268**, 11868 (1993); N. Okamoto *et al.*, *ibid.* **269**, 1231 (1994).
2. R. M. Duvoisin, C. Zhang, K. Ramonell, *J. Neurosci.* **15**, 3075 (1995).
3. S. Nakanishi, *Science* **258**, 597 (1992); R. Shigemoto *et al.*, *J. Neurosci.* **17**, 7503 (1997).
4. R. Shigemoto *et al.*, *Neuron* **12**, 1245 (1994); A. Aiba *et al.*, *Cell* **79**, 365 (1994); A. Aiba *et al.*, *ibid.*, p. 377; M. Kano *et al.*, *Neuron* **18**, 71 (1997).
5. E. M. Brown *et al.*, *Nature* **366**, 575 (1993).
6. J. E. Garrett *et al.*, *J. Biol. Chem.* **270**, 12919 (1995).
7. K. Kubokawa *et al.*, *FEBS Lett.* **392**, 71 (1996).
8. Complementary RNA for injection into oocytes was prepared with an in vitro transcription kit (Stratagene), and the yield was estimated by loading cRNA onto an agarose gel. Noninjected oocytes were used as a negative control. Preparation of *Xenopus* oocytes and the two-electrode voltage clamp experiments were carried out as described (*7*). The standard saline solution for culturing oocytes contained 88 mM NaCl, 1 mM KCl, 0.3 mM $Ca(NO_3)_2$, 0.41 mM $CaCl_2$, 0.8 mM $MgSO_4$, 2.4 mM $NaHCO_3$, and 15 mM Hepes (pH 7.6). In the experiments of Fig. 1, A and B, Fig. 2, A and B, Fig. 3, A, B, and D, and Fig. 5, the Ca^{2+}-free saline (0 mM Ca^{2+}, 0.3 mM Mg^{2+}), which contained 88 mM NaCl, 1 mM KCl, 2.4 mM $NaHCO_3$, 0.3 mM $MgCl_2$, and 15 mM Hepes (pH 7.6), was used to reduce the basal level of the Ca^{2+}-Cl^- current. The concentration of Mg^{2+} was held at 0.3 mM to suppress the leak current level. The Ca^{2+}-Cl^- current was monitored by applying depolarizing pulses of 175 ms to 60 mV every 2 s from the holding potential of −80 mV. While the oocytes were being given the repeated depolarizing pulses, one-fifth volume of 5× concentrated stock solutions of polyvalent cations or glutamate was applied gently to the bath, so that the flow was not directed at the oocyte, and then mixed immediately and thoroughly with a pipette. In the experiments of Fig. 1C, a high-K^+ solution containing 90 mM KCl, 0.3 mM $MgCl_2$, and 10 mM Hepes (pH 7.5) was used.
9. D. Riccardi *et al.*, *Proc. Natl. Acad. Sci. U.S.A.* **92**, 131 (1995); M. Ruat *et al.*, *ibid.*, p. 3161.
10. Y. Kubo, T. Miyashita, Y. Murata, unpublished observation.
11. Y. Kubo, E. Reuveny, P. A. Slesinger, Y. N. Jan, L. Y. Jan, *Nature* **364**, 802 (1993); N. Dascal *et al.*, *Proc. Natl. Acad. Sci. U.S.A.* **90**, 10235 (1993); F. Lesage *et al.*, *J. Biol. Chem.* **270**, 28660 (1995).
12. Chimeric molecules were prepared as follows. A unique Eco RV site was introduced at the very end of the NH_2-terminal cytoplasmic region of mGluRs 1α, 2, and 3 by mutagenesis with Sculptor kit (Amersham). These mutations did not cause amino acid substitution in mGluR1α and caused one mutation in mGluR2 (A566I, in which Ala at position 566 is mutated to Ile) and in mGluR3 (A575I). These amino acid substitutions did not affect the responses. The introduced Eco RV sites were then used to prepare chimeric molecules R2(N)-R1 and R3(N)-R1. The point mutants in Fig. 3D were also prepared with Sculptor kit (Amersham), and the sequences of the primer regions were determined by a DNA sequencer (ABI 377). To avoid unexpected mutations, we confirmed that two independent clones of the same mutation showed identical properties.
13. P. J. O'Hara *et al.*, *Neuron* **11**, 41 (1993).
14. To minimize the glutamate concentration in the medium, we cultured CHO cells in glutamine-free Dulbecco's minimum essential medium (DMEM) (2 mM Ca^{2+}) and 10% dialyzed fetal bovine serum (Gibco). Instead of glutamine, GlutaMAX-1(Gibco) at a reduced concentration of 2 mM was added to the medium just before use and the medium was changed twice a day. Wild-type mGluR1α and the S166D mutant were subcloned into $pCXN_2$ expression vector [H. Niwa, K. Yamamura, J. Miyazaki, *Gene* **108**, 193 (1991)] and then transiently transfected into CHO cells with Lipofectamine Plus (Gibco). Forty-eight hours later, the living cells were observed or fixed with 4% paraformaldehyde and 0.2% picrinic acid for immunohistochemistry analysis. For observation of living cells, pEGFP (Clonetech) was cotransfected to identify transfected cells. For the experiment in Fig. 1D, a CHO cell line stably expressing mGluR3 was established by G418 (Gibco) selection.
15. The transfected cells were identified by staining with polyclonal antibody to mGluR1 (Chemicon) and Cy3-labeled secondary antibody (Jackson ImmunoResearch Labs, West Grove, PA). The morphology of the actin filaments was visualized by staining with fluorescein isothiocyanate (FITC)–labeled phalloidin.
16. I. Aramori and S. Nakanishi, *Neuron* **8**, 757 (1992).
17. P. M. Vassilev, J. Mitchel, M. Vassilev, M. Kanazirska, E. M. Brown, *Biophys. J.* **72**, 2103 (1997).
18. The cAMP level of CHO cells expressing mGluR 2 or 3 were measured as follows. Cells were cultured in GlutaMAX-free medium for 4 hours, then rinsed by and incubated in the measurement solution (140 mM NaCl, 4 mM KOH, 10 mM Hepes, 0.3 mM $MgCl_2$, 1 mM isobutyl-methylxanthine) at 37°C for 20 min. Cells were then incubated in the measurement solution with 10 μM forskolin and a ligand (glutamate or Ca^{2+}) at 37°C for 10 min. Cells were lysed by 5% trichloroacetic acid, and the cAMP levels were measured by the cAMP EIA system (Amersham) following the manufacture's protocol. In the experiment of mGluR1α-expressing cells, forskolin was not added.
19. Single-letter abbreviations for the amino acid residues are as follows: A, Ala; C, Cys; D, Asp; E, Glu; F, Phe; G, Gly; H, His; I, Ile; K, Lys; L, Leu; M, Met; N, Asn; P, Pro; Q, Gln; R, Arg; S, Ser; T, Thr; V, Val; W, Trp; and Y, Tyr.

20. We thank S. Nakanishi for providing us with rat mGluRs 1α through 7 cDNA clones and CHO cell line expressing mGluR2; N. Sekiyama for teaching us techniques of cell culture and the cAMP measurement; M. Lazdunski and J. Miyazaki for GIRK2 cDNA and $pCXN_2$ vector, respectively; R. Murrell-Lagnado for comments on the manuscript; and K. Kubokawa, H. Okado, and K. Takahashi for discussion. Supported by research grants from the ministry of Education, Science, Sports and Culture of Japan for Exploratory Research to Y.K. and for scientific research on the priority area of "Channel-Transporter Correlation" to Y.K. Y.K. is also supported by Core of Research for Evolutional Science and Technology of the Japan Science and Technology Corporation.

18 November 1997; accepted 15 January 1998

Hyperinnervation of Neuromuscular Junctions Caused by GDNF Overexpression in Muscle

Quyen T. Nguyen,* Alexander Sh. Parsadanian,* William D. Snider, Jeff W. Lichtman†

Overexpression of glial cell line–derived neurotrophic factor (GDNF) by muscle greatly increased the number of motor axons innervating neuromuscular junctions in neonatal mice. The extent of hyperinnervation correlated with the amount of GDNF expressed in four transgenic lines. Overexpression of GDNF by glia and overexpression of neurotrophin-3 and neurotrophin-4 in muscle did not cause hyperinnervation. Thus, increased amounts of GDNF in postsynaptic target cells can regulate the number of innervating axons.

Experimental application of growth factors can alter the density and distribution of axon branches (*1*); hence, growth factor release may be one means by which target cells regulate the number of synaptic connections they receive (*2*, *3*). We sought to test this idea in a system where the complement of axon branches innervating a target cell could be visualized and functionally assessed. We generated mice in which muscle fibers synthesized excess amounts of a specific neurotrophic factor, GDNF, and studied innervation at the neuromuscular junction (NMJ). GDNF was chosen because it is perhaps the most potent survival factor for motor neurons, both in vitro and in vivo (*4*–*6*). In addition, GDNF is synthesized by muscle and Schwann cells (*4*, *7*, *8*) and is internalized and specifically transported retrogradely by motor neurons through a receptor-mediated process (*6*).

To examine the effect of increased target-derived GDNF on NMJ development, we generated several lines of *Myo-GDNF* mice (*9*) that overexpress GDNF under a muscle-specific (myogenin) promoter (*10*, *11*) (Fig. 1A). The myogenin promoter was chosen because it drives transgene expression in muscle beginning in embryogenesis, about the time axons first approach muscle fibers, and continues expression into postnatal life (*10*).

Q. T. Nguyen and J. W. Lichtman, Department of Anatomy and Neurobiology, Washington University School of Medicine, St. Louis, MO 63110, USA.
A. Sh. Parsadanian and W. D. Snider, Department of Neurology, Washington University School of Medicine, St. Louis, MO 63110, USA.

*These authors contributed equally to this report.
†To whom correspondence should be addressed. E-mail: jeff@thalamus.wustl.edu

Ten founder lines integrated the transgene *Myo-GDNF* (Fig. 1B) (9). On the basis of the amount of mRNA detected on postnatal day 1 (P1) (*12*), four of the 10 lines were chosen for further study: the two with the highest expression of GDNF mRNA (lines 8658 and 7301) (Fig. 1, D, E, G, and H) and two with GDNF mRNA expression that was indistinguishable from that of the wild type (as control). These four lines were compared to wild-type littermates (Fig. 1, C and F). Because the overexpression of GDNF mRNA and protein is greater in line 8658 than in line 7301, these two high-expressing lines are denoted *Myo-GDNF* (high) and *Myo-GDNF* (low), respectively. In the two high-expressing lines but not in control muscles, quantities of GDNF protein at P3 as measured by enzyme-linked immunosorbent assay (ELISA) (*13*) were elevated and paralleled the increases in mRNA expression (Table 1).

Table 1. Comparison of GDNF mRNA and protein expressed by neonate and adult (4 to 5 months) wild-type, *Myo-GDNF* (low), and *Myo-GDNF* (high) mice.

Age	Wild type	*Myo-GDNF* (low)		*Myo-GDNF* (high)	
		Total	Transgenic	Total	Transgenic
P1 GDNF mRNA (grains/250 μm^2)	30.6 ± 2.0	99.2 ± 3.7	68.6	269.8 ± 22.0	239.2
P3 GDNF protein (pg/mg protein)	24.4	44.4	19.6	88.8	64.5
Adult GDNF protein (pg/mg protein)	30.5	45.6	15.1	83.6	53.1

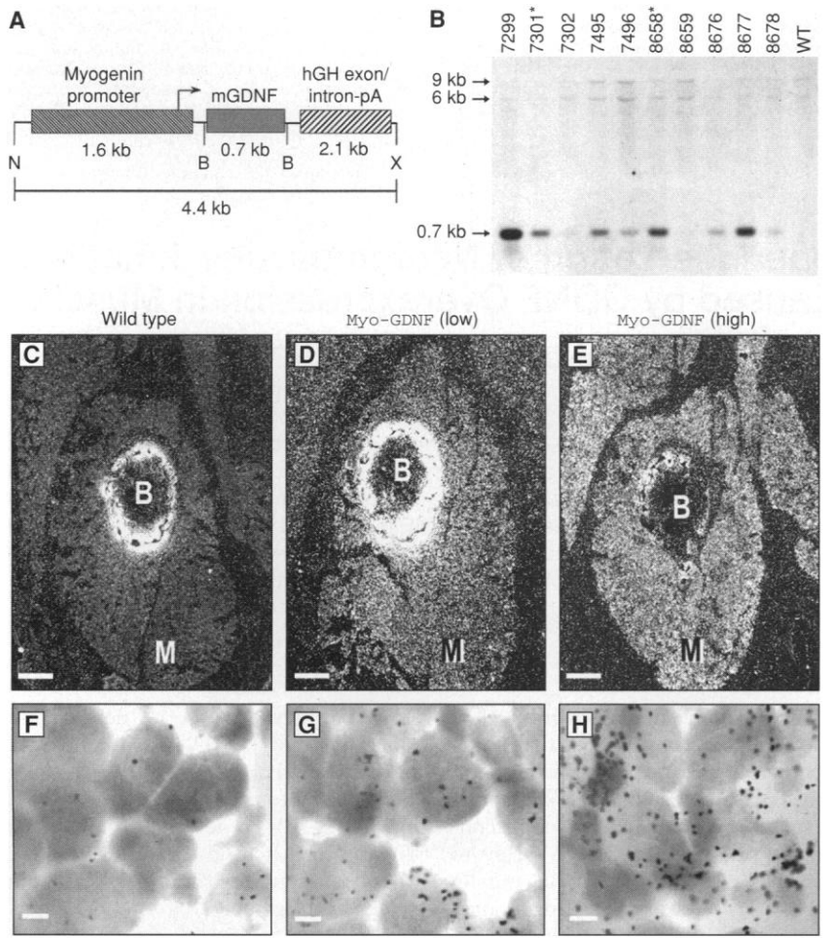

Fig. 1. (**A**) Schematic of *Myo-GDNF* transgene construct. The 4.4-kb construct contains 1.6 kb of myogenin promoter, 0.7 kb of mouse GDNF (mGDNF) cDNA, and 2.1 kb of human growth hormone (hGH) gene including polyadenylation signal (pA). N, Not I; B, Bam HI; X, Xho I. (**B**) Southern blot analysis of *Myo-GDNF* transgenic lines. The 0.7-kb band corresponds to transgene GDNF cDNA. The 6- and 9-kb bands correspond to the endogenous GDNF gene. Progeny from lines 7301 and 8658 (asterisks) were used for the remaining studies. (**C** to **E**) Low-power dark-field photomicrographs of in situ hybridization at the level of the forelimb of P1 pups from *Myo-GDNF* transgenic lines *Myo-GDNF* (low) and *Myo-GDNF* (high), and wild-type littermates with a probe specific for GDNF mRNA. The white ring in the center (B) is artifactual hybridization to bone. The wild type and the two different transgenic lines show differing extents of GDNF mRNA expression in developing muscles (M). Scale bars, 200 μm. (**F** to **H**) High-power bright-field views of silver grains [from the same sections as (C) to (E)]. Grains are specific for muscle cells. Scale bars, 5 μm.

Neuromuscular innervation was studied at multiple time points between birth and adulthood in all four transgenic lines and in wild-type animals. Normally in mammals, two or more motor axons innervate each NMJ at birth, but this number decreases to one over the first several postnatal weeks because of synapse elimination and associated axonal branch withdrawal (*14*). However, innervation of NMJs in the *Myo-GDNF* (high) and *Myo-GDNF* (low) mice was abnormal in several ways during the first several postnatal weeks. First, there were many more converging axons than normal (*15*) (Fig. 2). At some junctions, the number of inputs was several times the highest number of innervating axons observed in age-matched wild-type animals (Fig. 3). Despite the increased innervation, there was still only one NMJ on each muscle fiber, as in control muscles (Fig. 2). Second, in addition to the increase in the number of converging axons, the period of multiple innervation persisted longer than normal, doubling from 2 weeks to 1 month in *Myo-GDNF* (high) mice (Fig. 3A). Interestingly, when NMJs in overexpressing muscles had lost on average all but two axons, the transition to single innervation was approximately as fast as in control animals when they were similarly innervated (Fig. 3A).

The prolonged period of multiple innervation in these animals did not appear to be caused by a systemic maturational delay: Although the transgenic animals' weight tended to be slightly lower than that of control littermates during the first few postnatal weeks (90% of control at P0, 85% at P8, 70% at P14, and 83% at P23), eye opening, fur growth, weaning, and reproduction all occurred at appropriate times. We found that by adulthood, amounts of GDNF protein from the transgene dropped somewhat in both *Myo-GDNF* (high) and *Myo-GDNF* (low) mice (Table 1). Thus, we do not yet know if the eventual loss of multiple axonal convergence could be prevented altogether by maintained elevation of GDNF. The observed hyperinnervation

appeared to be related to the dose of GDNF because both the number of converging axons per multiply innervated endplate and the time required for an entire muscle to become uniformly singly innervated correlated with the amount of GDNF expressed in the *Myo-GDNF* (high) and *Myo-GDNF* (low) lines (Fig. 3A).

To determine whether GDNF overexpression may have induced innervation of muscle fibers by sensory or autonomic axons, which express the GDNF receptor Ret (*16*) but would not be expected to be functional, we recorded synaptic responses from diaphragm muscle fibers of transgenics and wild-type controls while stimulating the phrenic nerve with varying voltages (*17*). At P9 to P10, 80% of muscle fibers (n = 51, three animals) in the *Myo-GDNF* (high) line were multiply innervated. Of these, 56% (23 of 41) were contacted by two axons, and 44% (18 of 41) were contacted by three or more axons (Fig. 4). In some cases, we found that as many as three inputs to a muscle fiber were sufficiently strong to drive the muscle fiber to contract (Fig. 4, inset). In contrast, only 20% of muscle fibers (n = 55, two animals) in wild-type controls were multiply innervated, and in all cases by two axons. Therefore, the extra axonal inputs form functional contacts and almost certainly arise from motor neurons.

The hyperinnervation of muscle found in *Myo-GDNF* mice could have arisen because of a greater number of motor neurons innervating the muscle as a whole (as might occur if GDNF spared motor neurons from naturally occurring cell death) or because of a greater number of axonal branches in the innervating nerve. However, retrograde labeling of the motor neurons innervating the sternomastoid muscle with Fluoro-Gold (*18*) at P11 and counts of myelinated axons in the nerve to the sternomastoid at P9 to P10 (*19*) showed that the number of motor neurons or axon branches was only slightly higher in *Myo-GDNF* mice than in wild-type animals (Table 2). Thus, it seems more likely that the hyperinnervation is a consequence of more axonal branching within the muscle (that is, larger motor units).

Motor unit sizes were determined from twitch tension measurements at P10 (*20*). Maximal muscle tension was elicited in *Myo-GDNF* (high) animals by activation of only 66% of the number of motor axons needed to elicit maximal muscle tension in wild-type controls, indicating a greater degree of overlap in muscle fiber innervation by different axons (Table 2). Because excess GDNF did not alter the number of muscle fibers (Table 2), we conclude that motor units in P10 *Myo-GDNF* transgenic mice are at least 1.5 times the size of those in wild-type mice, and that these motor axons coinnervate the same NMJs more often than in wild-type mice.

During the period of greatest hyperinnervation (birth to 3 weeks postnatal), *Myo-GDNF* mice exhibit a tremor (Fig. 5). At neonatal ages, the shaking is sufficiently obvious that transgenic animals can be distinguished from their littermates without error. The tremor severity wanes as multiple innervation diminishes. The magnitude of the tremor was greater in amplitude and persisted over a longer developmental period in the *Myo-GDNF* (high) line than in the *Myo-GDNF* (low) line. Normal rodent neonates have a tremor that is most obvious during the first few postnatal days and gradually subsides over the next week (*21*). This tremor may be analogous to "jitteriness" in human neonates (*22*). Tremor disappearance corresponded to the loss of multiple innervation in each transgenic line, as it did in wild-type animals (*23*). The tremor therefore may be a reflection of the large number of muscle fibers innervated by each axon during early development, such that each motor axon impulse resulted in an obvious muscle twitch.

Muscle-specific overexpression of neurotrophin-3 (NT-3) with the myogenin promoter (*Myo–NT-3*) did not cause extra innervation of muscle fibers at the NMJ (*24*), even though motor neurons expressed the NT-3 receptor trkC and responded to NT-3 with increased survival (*25–27*) and even though these animals had an increased number of proprioceptive sensory axons and target muscle spindles (*11*). Muscle-specific overexpression of NT-4 (*Myo–NT-4*) also did not cause extra innervation of muscle fibers (*24*), even though motor neurons express the trkB receptor (*26–28*) and NT-4 causes sprouting in adult rodents (*29*).

Fig. 2. NMJs in mice expressing *Myo-GDNF* are hyperinnervated during development. Images are low-power fluorescence photomicrographs of sternomastoid muscles from a wild-type mouse (**A**) and a *Myo-GDNF* (high) mouse (**B**) at P8. Individual muscle fibers are running diagonally from top right to bottom left; postsynaptic AChRs are labeled red with TRITC-αBTX, and presynaptic axon neurofilaments and nerve terminal synaptophysin are immunolabeled green. Nerve terminals overlying AChRs at the NMJ appear yellow. The majority of muscle fibers in the wild-type animal are contacted by only one axon at this age. Note the axon in the process of being eliminated, which appears as a retracting bulb (*). The majority of muscle fibers in the *Myo-GDNF* (high) animal are multiply innervated, often by three or more axons. Scale bar, 10 μm.

Table 2. Comparison of the numbers of motor neurons, axons, muscle fibers, and motor units in wild-type and *Myo-GDNF* (high) mice (n.s., not significant).

Quantity	Wild type	*Myo-GDNF* (high)	Difference (%)	Significance
Number of motor neurons (P11)	81.5 ± 9.1 (n = 6)	94.0 ± 7.2 (n = 3)	115.3	n.s.
Number of axons (P9, P10)	136, 130 (n = 2)	150 ± 5.8 (n = 3)	112.8	n.s.
Number of muscle fibers (P11, P12)	1354, 1346 (n = 2)	1283, 1457 (n = 2)	101.5	n.s.
Number of motor units to maximal tension (P10)	56.0 ± 2.3 (n = 8)	36.8 ± 1.65 (n = 4)	65.7	P = 0.0003

The source of excess GDNF affects the amount of hyperinnervation. Overexpression of GDNF by glial cells under the glial fibrillary acidic protein (GFAP) promoter (*30*) had no effect on the number of axons converging on muscle fibers or the time course of synapse elimination, even though motor neurons in these animals are less susceptible to axotomy-induced cell death as a consequence of GDNF (*31*). However, we do not yet know whether glial cells at the NMJ (terminal Schwann cells) express the *GFAP-GDNF* transgene.

The hyperinnervation seen with muscle-specific overexpression of GDNF is more extreme than that described after parenteral administration of neurotrophins and other neurotrophic factors. These previous manipulations had modest effects on the time course of synapse elimination and had no effect on the number of innervating axons each target cell received (*32*). The effect with muscle-derived GDNF is also more pronounced than that seen in the mutant mouse *paralysé*, in which a deficit in neuromuscular activity is thought to delay synapse elimination but apparently does not cause extra axonal convergence (*33*).

It is not known how GDNF causes hyperinnervation. Muscle-derived GDNF may act as a synaptotrophin to prolong the maintenance of synaptic connections that were established during early development (*3*). Alternatively, GDNF may have caused hyperinnervation by inducing motor axons to establish extra terminal branches that are capable of forming synapses. In the latter case, the period of multiple innervation might be prolonged because of the additional time necessary to eliminate the abnormally large number of axons at each NMJ. In either case, our results demonstrate that enhanced trophic factor expression by postsynaptic cells can increase the amount of innervation they receive. Moreover, this synaptic plasticity is mediated by a growth factor outside the prototypical neurotrophin family.

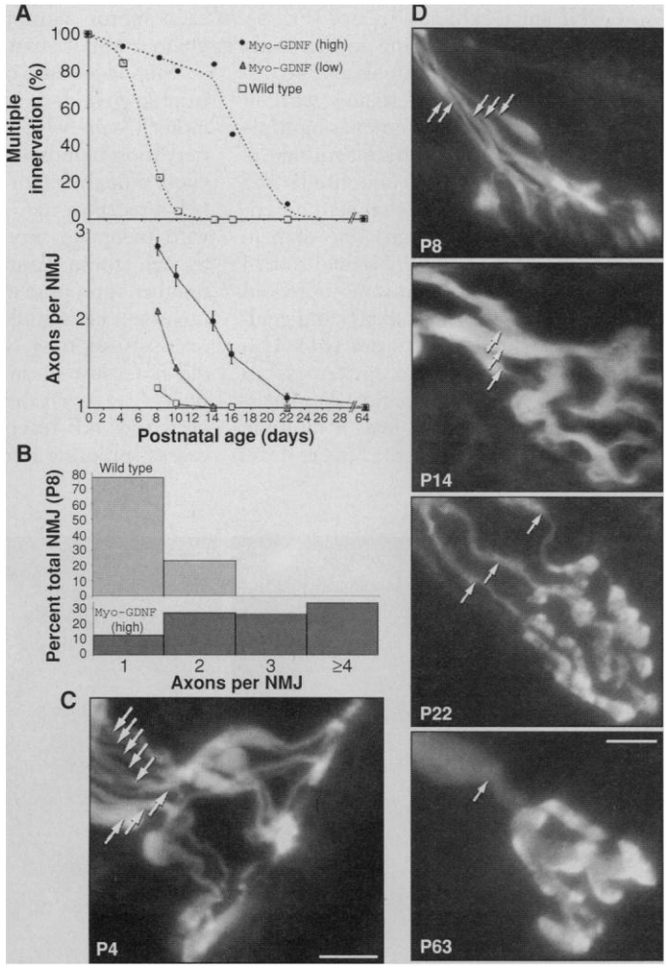

Fig. 3. (**A**) Delay of synapse elimination. Upper panel: NMJs in mice expressing *Myo-GDNF* are innervated by more than one motor axon (multiply innervated) for a longer period of development than are junctions in normal mice. Axons innervating the sternomastoid muscle in *Myo-GDNF* overexpressors (solid circles) and wild-type (open squares) littermates were immunolabeled with antibodies to neurofilament and synaptophysin and were viewed by confocal microscopy. The results show a delay of about 2 weeks in the loss of multiple innervation for the *Myo-GDNF* (high) line. Lower panel: Graph of the average number of axons converging to innervate single muscle fibers as a function of postnatal age, showing a dose dependence of hyperinnervation on the amount of GDNF for wild-type, *Myo-GDNF* (low), and *Myo-GDNF* (high) animals. (**B**) Bar graph showing distribution of axons per NMJ at P8 in wild-type and *Myo-GDNF* (high) animals. (**C** and **D**) Examples of confocal images of immunolabeled axons converging to single NMJs for *Myo-GDNF* animals during the first two postnatal months. Relative to age-matched control mice, muscle fibers in young mice expressing *Myo-GDNF* are innervated by more axons. In (C), an NMJ innervated by eight axons (arrows) at P4 is shown; this number of converging axons is greater than we have observed in normal animals at any postnatal age. Scale bar, 5 μm. In (D), examples of NMJs at different postnatal ages are shown: P8 (NMJ with five converging axons), P14 (NMJ innervated by three axons), P22 (endplate innervated by three axons), and P63 (100% of muscle fibers are singly innervated). Scale bar, 5 μm (P8–P22), 8.3 μm (P63).

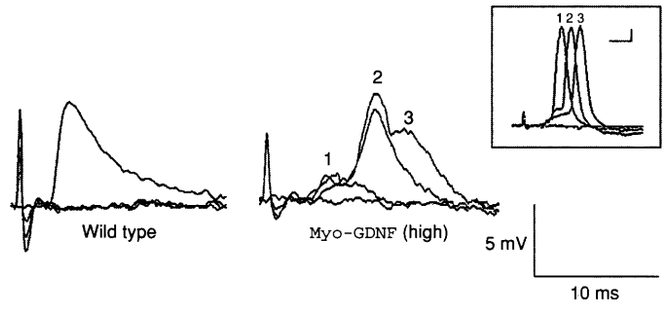

Fig. 4. Extra innervation of muscle fibers in *Myo-GDNF* overexpressors is functional. Examples of intracellular recording traces of synaptic potentials elicited by gradual recruitment of motor axon innervation by progressively increasing the strength of stimulus to the phrenic nerve. Superimpositions of traces from a diaphragm muscle fiber are shown for wild-type and *Myo-GDNF* (high) mice at P9. Graded stimulation of the phrenic nerve evoked a single endplate potential from the wild-type fiber, indicating that the muscle fiber is singly innervated. Graded stimulation of the phrenic nerve evoked three distinct endplate potentials from the *Myo-GDNF* muscle fiber, indicating that the fiber is innervated by three separate axons. All three of these axons were capable of driving the muscle fiber to threshold (insert; scale represents 5 mV, 5 ms).

Fig. 5. *Myo-GDNF* animals display an activity-dependent high-frequency tremor during the period of hyperinnervation. The photograph (exposure, 1 s) shows a P4 *Myo-GDNF* mouse standing next to its wild-type littermate.

REFERENCES AND NOTES

1. R. J. Cabelli, A. Hohn, C. J. Shatz, *Science* **267**, 1662 (1995); S. Cohen-Cory and S. E. Fraser, *Nature* **378**, 192 (1995); P. Caroni and M. Becker, *J. Neurosci.* **12**, 3849 (1992); P. Caroni and P. Grandes, *J. Cell Biol.* **110**, 1307 (1990).
2. C. G. Causing *et al.*, *Neuron* **18**, 257 (1997).
3. W. D. Snider and J. W. Lichtman, *Mol. Cell. Neurosci.* **7**, 433 (1996).
4. C. E. Henderson *et al.*, *Science* **266**, 1062 (1994).
5. L. J. Houenou, R. W. Oppenheim, L. X. Li, A. C. Lo, D. Prevette, *Cell Tissue Res.* **286**, 219 (1996).
6. Q. Yan, C. Matheson, O. T. Lopez, *Nature* **373**, 341 (1995).
7. D. E. Wright and W. D. Snider, *Cell Tissue Res.* **286**, 209 (1996).
8. M. Yamamoto, G. Sobue, K. Yamamoto, S. Terao, T. Mitsuma, *Neurochem. Res.* **21**, 929 (1996).
9. A mouse GDNF cDNA was cloned by the reverse transcription polymerase chain reaction (RT-PCR) using total RNA from embryonic (E13) head as template. A 700-bp Bam HI fragment, containing the full-length cDNA for mouse GDNF, was cloned into the plasmid cassette pMyo-hGH, containing a 1.6-kb Hind III–Kpn I fragment, corresponding to myogenin promoter (*10*–*11*), and a 2.1-kb Bam HI–Hind III fragment, containing human growth hormone gene including a polyadenylation signal. The resulting plasmid pMyo-GDNF was digested with Not I and Xho I; the 4.4-kb transgene fragment was eluted from an agarose gel and used for pronuclear injection (B6/CBA strain). Integration of the transgene into the mouse genome was determined by PCR on genomic DNA from mouse tail using the 5′-oligo (5′-TGATGTGGTAGTGGTAGGTCT-3′) and the 3′-oligo (5′-CAGGCATATTGGAGTCACTGG-3′). Genotype was confirmed by Southern (DNA) blot analysis as described (*11*) using a 0.7-kb digoxigenin-labeled PCR product, corresponding to the mouse GDNF cDNA as a probe.
10. T. C. Cheng, T. A. Hanley, J. P. Mudd, *J. Cell Biol.* **119**, 1649 (1992); J. P. Merlie, J. Mudd, T. C. Cheng, E. N. Olson, *J. Biol. Chem.* **269**, 2461 (1994).
11. D. E. Wright, L. Zhou, J. Kucera, W. D. Snider, *Neuron* **19**, 503 (1997).
12. The amount of GDNF mRNA in the muscle of F_1 offspring from different transgenic lines was assessed by in situ hybridization on cryostat sections (16 μm) of P1 mice cut in the transverse plane at the level of the forelimbs using riboprobes to GDNF, as described (*7*).
13. Amounts of GDNF protein in muscle homogenate were measured using the GDNF E_{max} immunoassay kit (Promega), following the manufacturer's instructions using whole muscles (upper hind limbs) dissected from P3 and adult animals.
14. Q. T. Nguyen and J. W. Lichtman, *Curr. Opin. Neurobiol.* **6**, 104 (1996).
15. Mice were anesthetized and a ventral midline incision was made to expose sternomastoid muscles. Tetramethyl rhodamine isothiocyanate α-bungarotoxin (TRITC-αBTX, 5 μg/ml; Molecular Probes) was applied to the muscles (20 min) to label postsynaptic acetylcholine receptors (AChRs). After transcardial perfusion with 2% paraformaldehyde, whole sternomastoid muscles were dissected and pinned on a Sylgard-lined dish. Nerve terminals and axons were labeled with antibodies to neurofilament (SMI312, Sternberger) and synaptic vesicles (G95, P. Greengard). NMJs doubly labeled for nerve terminals and AChRs were viewed with high-numerical-aperture objectives with confocal optics using a real-time scanner (Noran, Odyssey). The number of incoming axons could be accurately defined by carefully focusing through the region of the NMJ where the nerves enter.
16. T. Tsuzuki *et al.*, *Oncogene* **10**, 191(1995); D. C. Molliver *et al.*, *Neuron* **19**, 849 (1997).
17. Whole diaphragm muscles with an intact portion of the phrenic nerve were dissected from P9–P10 mice in oxygenated culture medium (Dulbecco's). Electrophysiological recordings of numbers of axons innervating single muscle fibers were made using intracellular recording as described [P. A. Redfern, *J. Physiol. (London)* **209**, 701 (1970)] in the presence of 1 to 3 μM curare to prevent muscle contraction.
18. P6–P8 mice were anesthetized and a ventral midline incision was made to expose the left sternomastoid muscle. Motor neurons that innervate the sternomastoid muscle were retrogradely labeled with Fluoro-Gold (Fluorochrome) as described [D. M. Rotto-Percelay *et al.*, *Brain Res.* **574**, 291 (1992)]. Briefly, three separate injections (200 to 400 nl) of 4% Fluoro-Gold in saline were made into the left sternomastoid muscle. The wound was sutured closed and the mouse pups were returned to their mother. At P11 (3 to 5 days later), the pups were reanesthetized; brainstem and spinal cords were processed for motor neuronal cell counting with the following changes: Brainstem and spinal cords were cut in the horizontal plane at 12 μm, mounted serially on glass slides, counterstained with ethidium bromide [L. C. Schmued, L. W. Swanson, P. E. Sawchenko, *J. Histochem. Cytochem.* **30**, 123 (1982)], and coverslipped in glycerin. Fluoro-Gold–labeled neurons were examined with a fluorescence microscope with an ultraviolet filter set (Leica) and imaged with a silicon-intensified camera. As a precaution to prevent errors associated with double counting, only cells in which a nucleus could be seen were counted and adjacent sections were compared [physical dissector; R. E. Coggeshall, *Trends Neurosci.* **15**, 9 (1992)].
19. P9–P10 mice were perfused transcardially with 2% paraformaldehyde. The nerve to the sternomastoid muscle was dissected and stored in a 2% paraformaldehyde–2% glutaraldehyde solution for 5 to 6 hours. After an overnight rinse in 5% sucrose in phosphate-buffered saline, nerves were stained in 1% osmium tetroxide. Plastic sections (1 μm) were serially mounted and stained with 1% toluidine blue–1% sodium borate. Cross sections of the nerve were photographed under a dissecting scope (50×) and the number of myelinated axons (of all diameters) counted.
20. Whole sternomastoid muscles with an intact portion of the incoming nerve were dissected from P10 mice in oxygenated culture medium (Dulbecco's). Motor unit twitch tension recordings using a force transducer (Cambridge Neuroscience) were performed as described [W. J. Betz, J. H. Calwell, R. R. Ribchester, *J. Physiol. (London)* **297**, 463 (1979)].
21. M. R. Pranzatelli, *Clin. Neuropharmacol.* **13**, 329 (1990).
22. N. P. Rosman, J. H. Donelly, M. A. Braun, *J. Dev. Behav. Pediatr.* **54**, 263 (1984).
23. M. C. Brown, J. K. Jansen, D. Van Essen, *J. Physiol. (London)* **261**, 387 (1976); T. Fladby, *Acta Physiol. Scand.* **129**, 229 (1987).
24. Q. T. Nguyen, J. W. Lichtman, A. Sh. Parsadanian, W. D. Snider, data not shown.
25. R. W. Oppenheim, *Neuron* **17**, 195 (1996).
26. Q. Yan *et al.*, *J. Neurobiol.* **24**, 1555 (1993).
27. C. E. Henderson *et al.*, *Nature* **363**, 266 (1993).
28. V. E. Koliatsos *et al.*, *Proc. Natl. Acad. Sci. U.S.A.* **91**, 3304 (1994).
29. H. Funakoshi *et al.*, *Science* **268**, 1495 (1995).
30. M. Brenner, W. C. Kisseberth, Y. Su, F. Besnard, A. Messing, *J. Neurosci.* **14**, 1030 (1994).
31. C. R. Keller-Peck, A. Sh. Parsadanian, L. Zhou, W. D. Snider, *Soc. Neurosci. Abstr.* **23**, 620 (1997).
32. Y. W. Kwon, S. J. Abbondanzo, C. L. Stewart, M. E. Gurney, *J. Neurobiol.* **28**, 35 (1995); C. L. Jordan, *Dev. Neurosci.* **18**, 185 (1996); A. W. English and G. Schwartz, *Dev. Biol.* **169**, 57 (1995).
33. B. Blondet *et al.*, *Dev. Biol.* **132**, 153 (1989).

34. We thank L. Worley for excellent technical assistance. Supported by grants from NIH and the Muscular Dystrophy Association.

23 October 1997; accepted 21 January 1998

Conservation of T Cell Receptor Conformation in Epidermal γδ Cells with Disrupted Primary V_γ Gene Usage

Caroline A. Mallick-Wood, Julia M. Lewis, Lauren I. Richie, Michael J. Owen, Robert E. Tigelaar,* Adrian C. Hayday*†

A feature that distinguishes γδ T cell subsets from most αβ T cells and B cells is the association of expression of single T cell receptor (TCR) γ and δ variable (V) region gene segments with specific anatomic sites. Mice lacking the TCR $V_\gamma5$ chain normally expressed by most dendritic epidermal T cells were shown to retain a conformational determinant (idiotype) ordinarily expressed exclusively by such $V_\gamma5^+$ cells. Conservation by shuffled γδ TCR chains of an idiotype associated with a specific anatomic site indicates that for TCRγδ, as for immunoglobulin, conformation is associated to a greater extent with the function or development of lymphocyte repertoires than is the use of particular gene segments.

The efficacy of the adaptive immune system depends on its capacity to recognize pathogens in a highly antigen-specific manner. B cells and αβ T cells recognize antigens through surface immunoglobulin (Ig) and TCRs, respectively. Although γδ cells regulate immune responses to protozoal, bacterial, and viral infection (*1*, *2*), neither their primary physiological functions nor their antigen specificities have been fully clarified.

A characteristic feature of γδ cells is the association of single γ and δ chains with γδ cell subsets in specific anatomic sites. For example, most human peripheral blood γδ cells express $V_\gamma9$ and $V_\delta2$ chains of relatively limited diversity (*3*). More extreme examples occur in murine epithelia. Essentially all reproductive tract γδ cells express a canonical $V_\gamma6$-$V_\delta1$ TCR, whereas 60 to >99% of dendritic epidermal T cells (DETCs)—variation depending on strain and age of the mice—express a canonical $V_\gamma5$-$V_\delta1$ TCR (*4*), which can be detected with the monoclonal antibody (mAb) 17D1 (*5*). Ordinarily, 17D1 does not react